Enhanced siRNA Delivery and Silencing Gold–Chitosan Nanosystem with Surface Charge-Reversal Polymer Assembly and Good Biocompatibility

Lu Han,[†,§] Jing Zhao,[†,‡,§] Xu Zhang,[†] Weipeng Cao,[†] Xixue Hu,[†] Guozhang Zou,[†,*] Xianglin Duan,[‡,*] and Xing-Jie Liang[†,*]

[†]CAS Key Laboratory for Biomedical Effects of Nanomaterials and Nanosafety, National Center for Nanoscience and Technology, Beijing 100190, People's Republic of China and [‡]Laboratory of Molecular Iron Metabolism, College of Life Science, Hebei Normal University, Shijiazhuang 050016, People's Republic of China. [§]These authors contributed equally to this work.

ABSTRACT A simple nanocarrier coated with chitosan and the pH-responsive charge-reversible polymer, PAH-Cit, was constructed using layer-by-layer assembly to deliver siRNA. Gold nanoparticles (AuNPs) were directly reduced and stabilized by chitosan (CS), forming a positively charged AuNP-CS core. Charge-reversible PAH-Cit and polyethylenimine (PEI) were sequentially deposited onto the surface of AuNP-CS through electrostatic interaction, forming a PEI/PAH-Cit/AuNP-CS shell/core structure. After loading siRNA, the cytotoxicity of siRNA/PEI/PAH-Cit/AuNP-CS against HeLa and MCF-7R cells was negligible. This vehicle completely protected siRNA against enzymatic degradation at vector/RNA mass ratios of 2.5:1 and above. An *in vitro* release profile demonstrated an efficient siRNA release (79%) from siRNA/PEI/PAH-Cit/AuNP-CS at pH 5.5, suggesting a pH-induced charge-reversing action of PAH-Cit. This mechanism also worked *in vivo* and facilitated the escape of siRNA from endosomes. Using this carrier, the uptake of cy5-siRNA by HeLa cells was significantly increased compared to PEI, an efficient polycationic transfection reagent. In drug-resistant MCF-7 cells, specific gene silencing effectively reduced expression of *MDR1*, the gene encoding the drug exporter P-gp, and consequently promoted the uptake of doxorubicin. This simple charge-reversal polymer assembly nanosystem has three essential benefits (protection, efficient uptake, and facilitated escape) and provides a safe strategy with good biocompatibility for enhanced siRNA delivery and silencing.

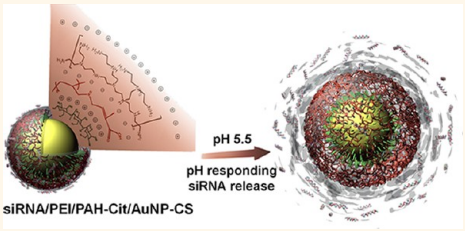

KEYWORDS: siRNA · layer-by-layer assembly · charge-reversible

Small interfering RNAs (siRNA), a new generation of biodrugs, can be utilized for silencing a wide range of target genes to treat a variety of diseases, including cancers.[1,2] However, the delivery of naked siRNA to the appropriate site remains a considerable hurdle owing to rapid enzymatic digestion, limited translocation through cellular membranes, and inefficient release from endosomes.[3] Therefore, one of the major challenges in siRNA therapy is to find a suitable gene delivery vehicle, the main features of which for clinical application are low toxicity and high transfection efficiency.[4,5] One obvious strategy for nucleic acid delivery is through viral vectors,[6,7] but the issues of immunogenicity, carcinogenicity, and inflammation that are associated with viral vectors have inspired the parallel development of nonviral carriers based on cationic lipids and polymers. Cationic polymers are strongly favored because they have the advantages of being more stable, easier to manipulate, and more economical than cationic liposomes.[8–10] Among the cationic polymers currently used for siRNA delivery, polyethylenimine (PEI), every third atom of which is a protonable amino nitrogen, is an outstanding core for the design of more sophisticated devices.[5,11–13]

Layer-by-layer (LBL) self-assembly, introduced by Decher in 1991,[14] is widely used to deposit multiple layers of positively and negatively charged polymers onto surfaces of films[15] or nanoparticles.[16] Gold nanoparticles (AuNPs) possess several advantages for use as a core, including bioinertia, nontoxicity, ready synthesis, and easy functionalization,[17,18] which is why they provide extremely attractive scaffolds for the creation of transfection agents.[19,20] Elbakry *et al.*[21] developed the LBL assembly of two oppositely charged polyelectrolytes, siRNA and PEI, on AuNPs. However, the release of siRNA into the cellular cytoplasm was low, due to strong binding between AuNPs and siRNA. As mentioned above, inefficient escape of siRNA from endosomes remains the critical intracellular barrier

* Address correspondence to liangxj@nanoctr.cn, zougz@nanoctr.cn, xlduan0311@163.com.

Received for review June 4, 2012 and accepted July 27, 2012.

Published online July 27, 2012
10.1021/nn3024688

during the delivery process. Therefore, in our previous study,[22] we created PEI/PAH-Cit/PEI/AuNP-MUA, in which a charge-reversible polymer, poly(allylamine hydrochloride)-citraconic anhydride (PAH-Cit), is embedded into PEI-based AuNPs to facilitate the release of siRNA. As an anionic carboxylate-functionalized polymer, PAH-Cit is used to fabricate multilayer films,[23] which can be readily converted back to cationic poly(allylamine) by amide hydrolysis upon exposure to acidic environments, such as those found within late endosomes and lysosomes. The siRNA knockdown studies *in vitro* indicated high efficiency of the payload release due to the charge conversion of PAH-Cit.

Conventionally, the synthesis of AuNPs involves the process of reduction of Au(III) with trisodium citrate or sodium borohydride. In order to fabricate polymer-coated AuNPs as cores for LBL assembly systems, negatively charged 11-mercaptoundecanoic acid (MUA)[22] is first conjugated to AuNPs *via* Au−S bonding, and PEI can then be deposited onto the negatively charged MUA-coated AuNPs. To construct PEI/PAH-Cit/PEI/AuNP-MUA, at least five assembly steps are needed. During the LBL assembly process, parameters including the polyelectrolyte concentration, the contour length of the polyelectrolyte chain, and the ionic strength collectively affect aggregation of nanoparticles and the stability of the colloidal dispersion.[24−26] Here, we used a biocompatible method to synthesize AuNPs, in which the AuNPs were reduced and stabilized by chitosan, giving AuNP-CS, a substitute for PEI/AuNP-MUA as the core for LBL assembly. It is worth highlighting that chitosan can be protonated at its amino group, making AuNP-CS positively charged. PEI/PAH-Cit/AuNP-CS was fabricated in only three LBL assembly steps, and the nanoparticles showed improved monodispersity with no reduction in delivery efficacy.

Another problem to be solved is the toxicity of gene vectors. From our previous work, we know that the constituents of PEI/AuNP-MUA do not contribute to siRNA delivery, while PEI is highly cytotoxic due to membrane perturbation and chromosome aberrations.[27] Here, we replaced inner-layer PEI with chitosan, a natural, biocompatible, and biodegradable polymer. We reasoned that the fabrication of LBL nanoparticles with polymers that are biodegradable inside cells will most likely improve the biocompatibility of gene vehicles.

In this study, the LBL technique was employed to fabricate a pH-responsive siRNA deliver nanosystem, PEI/PAH-Cit/AuNP-CS, with good biocompatibility. We investigated siRNA binding affinities, stability, cytotoxicity, and *in vitro* delivery efficacy of siRNA/PEI/PAH-Cit/AuNP-CS. Evidence is provided that the delivery system is capable of pH-triggered siRNA release, which led to improved siRNA knockdown efficiency.

RESULTS

Characterization of PEI/PAH-Cit/AuNP-CS. PEI/PAH-Cit/AuNP-CS was assembled layer-by-layer through electrostatic interaction. Due to the unique polymeric cationic character of chitosan, AuNP-CS, as the core of the system, had a positively charged surface, which was ready for deposition of the anionic, pH-responsive, charge-reversible polymer, PAH-Cit, and subsequently positively charged PEI.

The two sequential reversals of zeta-potential indicated successful deposition of PEI and PAH-Cit onto the surface of AuNP-CS (Figure 1a). The absorption peak of localized surface plasmon resonance (LSPR) (Figure 1b) shifted from 527 to 530 nm after each assembly step at pH 7.4, whereas there was no plasmon absorbance peak in the range from 600 to 700 nm after deposition of polyelectrolytes, indicating that there was no aggregation of AuNP-CS. This was further confirmed by TEM imaging (Figure 1d). These results demonstrated that most nanoparticles remained dispersed. Thus, optimal particles for loading siRNA were obtained.

After each coating step, the diameters of the nanoparticles were determined by DLS and TEM (Figure 1c,d). The average hydrodynamic diameter of AuNP-CS in HEPES buffer was 46.9 nm with a poly dispersity index of 0.215 (Figure 1c). However, TEM imaging (Figure 1d) indicated that the diameter was around 21 nm, lower than the value derived from DLS. The discrepancy between the DLS and TEM results suggested that AuNPs were stabilized with a layer of chitosan molecules about 10 nm thick, which expanded in the aqueous phase and shrunk after being dried.

After successful assembly of PAH-Cit and subsequent addition of PEI, the hydrated diameter of the NPs increased to 74.2 and 88.5 nm, respectively. The vehicle, PEI/PAH-Cit/AuNP-CS, was then complexed with siRNA, the size of which increased to 94.5 nm (Figure 1c). Samples were then negatively stained with uranyl acetate and examined by TEM, so that the polymer shells appeared white against the stained background. High-magnification TEM images of PAH-Cit-coated AuNP-CS and PEI/PAH-Cit-encapsulated AuNP-CS showed that the nanoparticles had a cocoon-like structure (insets in Figure 1d), further indicating that the polyelectrolyte was successfully deposited on the surface of AuNP-CS.

siRNA Binding Affinities and Stability of the siRNA/PEI/PAH-Cit/AuNP-CS Complexes. The interaction between negatively charged siRNA and cationic vehicles is known to strongly influence the efficiency of loading nucleic acid cargos. To investigate the siRNA loading capability of PEI/PAH-Cit/AuNP-CS, we performed agarose gel electrophoresis at mass ratios of vectors to siRNA ranging from 0.63:1 to 10:1. Compared to naked siRNA, the migration of particle-bound siRNA was completely prevented at ratios higher than 2.5 (Figure 2a, top panel), indicating that the vectors bound siRNA strongly enough to resist dissociation during electrophoresis. The stabilities of siRNA/PEI/PAH-Cit/AuNP-CS

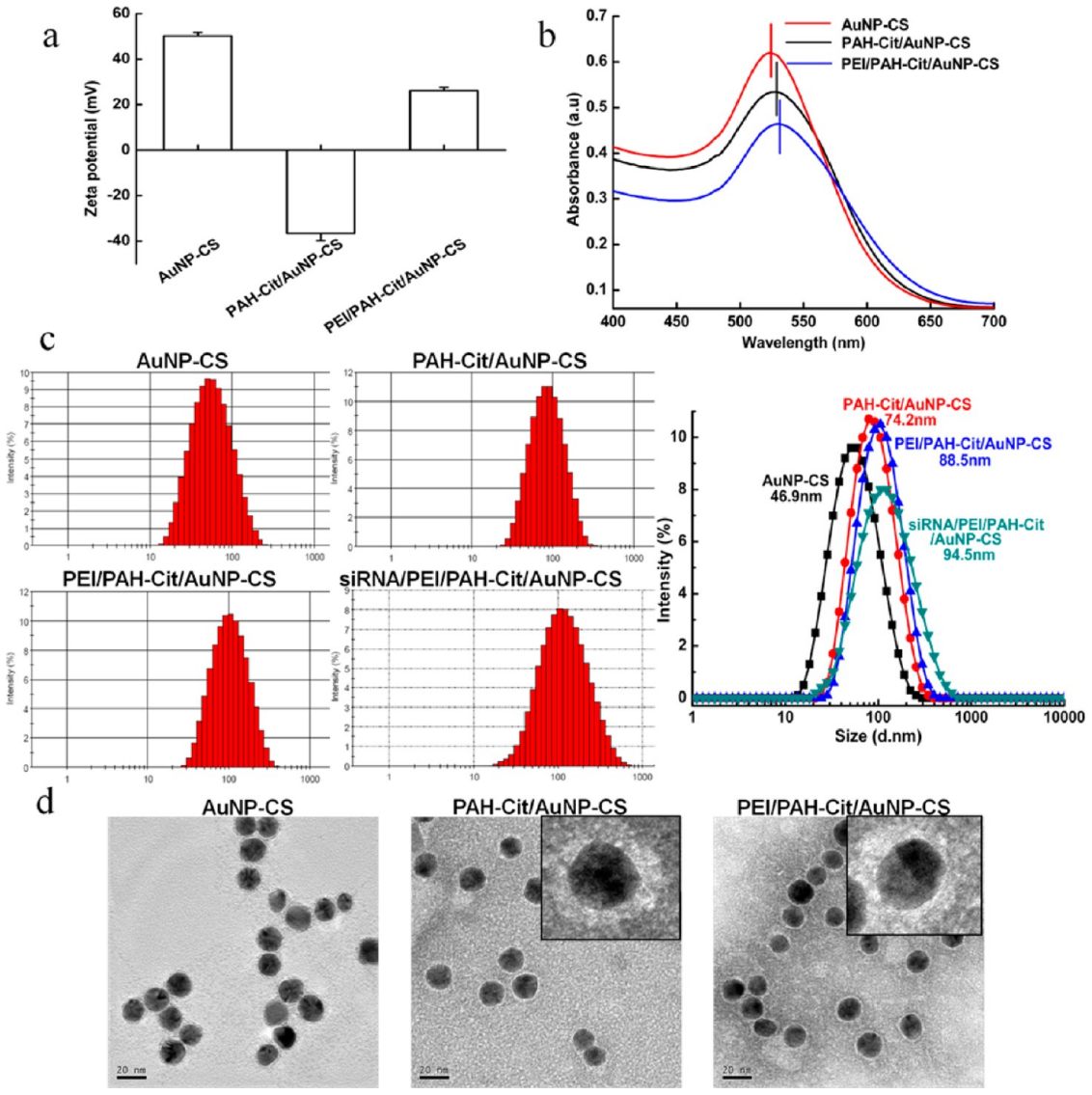

Figure 1. (a) Zeta-potential and (b) UV−vis spectra of PEI/PAH-Cit/AuNP-CS in 10 mM pH 7.4 HEPES buffer. (c) Representative hydrodynamic diameters of AuNP-CS, PAH-Cit/AuNP-CS,PEI/PAH-Cit/AuNP-CS, and siRNA/PEI/PAH-Cit/AuNP-CS determined by DLS at least three times. Average diameters were graphed by Origin software. (d) TEM images of AuNP-CS, PAH-Cit/AuNP-CS, and PEI/PAH-Cit/AuNP-CS. After each coating step, samples of PAH-Cit/AuNP-CS and PEI/PAH-Cit/AuNP-CS were dropped onto copper grids, allowed to dry, then negatively stained using 2% uranyl acetate and observed by TEM. Insets: Higher magnification micrographs of the assembled nanoparticles.

complexes were then examined by RNase digestion to mimic physiological conditions. Uncomplexed siRNA (Figure 2a, middle panel, lane 1) was detected with ethidium bromide stain. Once siRNA was either degraded by RNase (Figure 2a, middle panel, lane 2) or completely bound with gene vehicles (Figure 2a, middle panel, lanes 3−8), the ethidium bromide fluorescence disappeared. Figure 2a (middle panel, lanes 3−8) shows that the complexes with mass ratios from 0.63 to 1.25 partially prevented RNase digestion; nevertheless, when the ratio is above 1.25, RNase digestion was completely inhibited, indicating that siRNA is protected *via* association with the vehicles. Figure 2a (bottom panel) shows the release of siRNA by SDS replacement after RNase digestion. The fluorescence intensity gradually increased with the mass ratio from 0.63 to 10 (Figure 2a, bottom panel, lanes 3−8), further suggesting that released siRNA was protected by the vehicles of PEI/PAH-Cit/AuNP-CS instead of being degradated by RNase.

siRNA Release from the Complexes. To validate the functionality of charge-reversal of PAH-Cit, the PEI/PAH-Cit/AuNP/siRNA complexes were incubated at pH values of 5.5 and 7.4, and the amount of siRNA released into the supernatant was determined by measuring the absorbance at 260 nm using a Nanodrop spectrophotometer at different time points. After 4 h incubation, the cumulative siRNA release from the PAH-Cit complex reached 79% at pH 5.5 but only 23% at pH 7.4 (Figure 2b). The siRNA/PEI/PSS/AuNP-CS

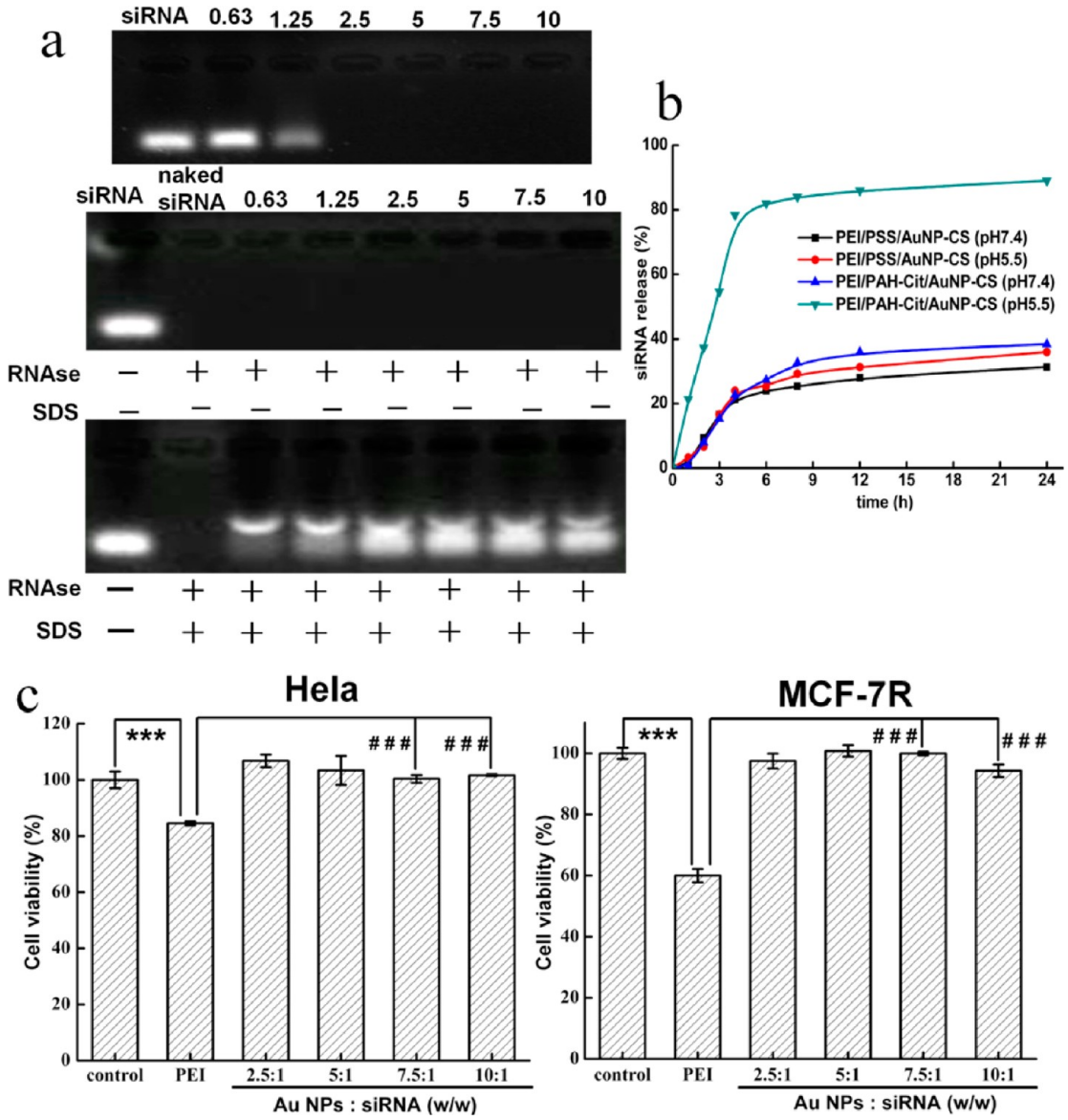

Figure 2. (a) Top panel: agarose gel retardation assay of siRNA/PEI/PAH-Cit/AuNP-CS complexes under various vector/siRNA mass ratios (0.63:1, 1.25:1, 2.5:1, 5:1, 7.5:1, and 10:1 from left to right). Middle panel: protection of siRNA against RNase digestion. Bottom panel: siRNA release from complexes by competitive binding of SDS with vehicles after enzymatic degradation. Naked siRNA was used as a control (first lane from the left). (b) Profile of siRNA release from siRNA/PEI/PAH-Cit/AuNP-CS complexes prepared at vector/siRNA mass ratios of 7.5:1 in pH 7.4 and pH 5.5 HEPES buffer at 37 °C. The percentage of cumulative siRNA release was measured at 0, 1, 2, 3, 4, 6, 8, 12, and 24 h. (c) Cytotoxicity of siRNA/PEI/PAH-Cit/AuNP-CS complexes at different vector/siRNA mass ratios was evaluated in HeLa and MCF-7R cells using a CCK-8 assay.

complex, in which PSS is not charge-reversible, had similar release curves at both pH 7.4 and pH 5.5, with only 36% siRNA released after 24 h (Figure 2b). This experiment demonstrated that the release of siRNA was facilitated by the charge-shifting character of PAH-Cit, which converted from anionic to cationic in the acidic environment and then disrupted the layer-by-layer structure of the complex.[23]

Cell Viability Assay. The biocompatibility of a delivery vector is critical for its potential application in clinical gene therapy. In this study, the cytotoxicity of siRNA/PEI/PAH-Cit/AuNP-CS complex on HeLa and MCF-7R cells was assessed using a CCK-8 cell viability assay. The viabilities of HeLa cells treated with the complex at various ratios were comparable to, or even higher than, the control (Figure 2c). Similarly, when MCF-7R cells were incubated with the complex for 48 h, no toxicity was observed (Figure 2c). However, PEI-25kD-treated HeLa and MCF-7R cells both showed significantly decreased viability compared with the control ($p < 0.001$). These results demonstrated the excellent biocompatibility of PEI/PAH-Cit/AuNP-CS. Mass ratios of this vector to siRNA ranging from 2.5 to 10 were chosen for subsequent transfection experiments.

siRNA Delivery Efficiency by PEI/PAH-Cit/AuNP-CS. To investigate the siRNA delivery efficacy by PEI/PAH-Cit/AuNP-CS,

confocal laser scanning microscopy (CLSM) and flow cytometry analysis were used to measure the uptake of cy5-labeled siRNA. HeLa cells were transfected with cy5-labeled siRNA complexed with PEI/PAH-Cit/AuNP-CS with mass ratios ranging from 2.5 to 10 and compared to siRNA-PEI complex with a N/P ratio of 10 (Figure 3a). AuNP-CS, the core of the vector alone without PEI/PAH-Cit modification, showed no siRNA delivery. In order to investigate *in vivo* whether PAH-Cit responds to pH change, reverses charge, and facilitates the release of siRNA from endosomes, PEI/PSS/AuNP-CS was used as a reference. The results were in agreement with intracellular siRNA uptake determined by Image-Pro Plus software (Figure 3b). The fluorescence intensities of cy5-siRNA delivered by the pH-responsive complex with mass ratios from 5 to 10 were all significantly higher than PEI and PEI/PSS/AuNP-CS (Figure 3c,d), which was in agreement with the confocal results. A vector/RNA mass ratio of 7.5:1 was the most effective for delivering cy5-siRNA into cells.

To confirm the enhanced endosomal escape of PEI/PAH-Cit/AuNP-CS, the intracellular distribution of assembled vectors was investigated by CLSM using cy5-labeled siRNA (Figure 4, left panels). After 6 h incubation with cy5-siRNA/PEI/PAH-Cit/AuNP-CS complexes, a majority of cy5-siRNA was dispersed in the cytoplasm. However, the cy5-siRNA delivered by PEI or PEI/PSS/AuNP-CS formed tight clusters and colocalized with lysosomes (Figure 4, middle and right panels), the yellow dots indicated by arrows in merged figures. We concluded that, compared with PEI/PSS/AuNP-CS and PEI, siRNA delivered by PEI/PAH-Cit/AuNP-CS escaped more efficiently from endosomes.

***In Vitro* Gene Silencing Efficacy of the PEI/PAH-Cit/AuNP-CS/siRNA Complex.** To evaluate siRNA transfection efficacy *in vitro*, we used a siRNA specifically targeting *MDR1*, the gene encoding P-glycoprotein (P-gp), which is overexpressed in multi-drug-resistant cell lines[28] such as MCF-7R. *MDR1* siRNA was delivered *via* PEI/PAH-Cit/AuNP-CS, and the level of MDR1 mRNA expression was measured by PCR. In cells treated with complexes with a mass ratio of 7.5, the *MDR1* mRNA level was reduced by nearly 80% (Figure 5a). Scrambled siRNA ("X" in Figure 5a) was used as a negative control to rule out any impact of the siRNA delivery method. Significant *MDR1* knockdown was seen with the siRNA/PEI/PAH-Cit/AuNP-CS treatment, compared to slight reduction with the siRNA/PEI treatment.

MCF-7R cells are resistant to anticancer agents like doxorubicin (dox) because P-gp is an efflux pump that exports a wide range of drugs. We test whether delivery of *MDR1* siRNA leads to reduction of the amount of dox being pumped out of MCF-7R cells. In this experiment, we used CLSM to analyze the uptake of dox by cells after they were pretreated for 48 h with *MDR1* siRNA complexed with different delivery vectors. Very faint dox fluorescence was visible after cells were treated with naked *MDR1* targeted siRNA (Figure 5b). No significant improvement in dox uptake was observed for *MDR1*-targeted siRNA complexed with PEI or with PEI/PSS/AuNP-CS. However, the intracellular dox concentration increased significantly after the cells were treated with the siRNA/PEI/PAH-Cit/AuNP-CS complex. The results of quantitative analysis performed by Image-Pro Plus software demonstrated that the dox uptake by MCF-7R cells treated with *MDR1* siRNA/PEI/PAH-Cit/AuNP-CS was more than twice over cells exposed to *MDR1* siRNA complex with PEI or PEI/PSS/AuNP-CS (Figure 5c), which were in accord with dox uptake evaluated by confocal imges (Figure 5b). These results further suggest that, due to the pH sensitivity of PAH-Cit, the delivery of *MDR1* targeted siRNA was markedly improved by PEI/PAH-Cit/AuNP-CS, which led to significant reduction of *MDR1* gene expression and the intracellular buildup of doxorubicin.

DISCUSSION

We previously reported that depositing a charge-reversal polyelectrolyte on gold nanoparticles creates a gene delivery nanosystem, which facilitates the escape of nucleic acids from endosomes/lysosomes.[22,29] The aim of this study was to construct a simple and biodegradable gene carrier using a facile assembly method, the siRNA delivery efficacy of which is comparable to the carriers designed in our previous work and superior to PEI.

Localization in the cytoplasm is the critical prerequisite of siRNA delivery to effectively silence specific cellular mRNAs. However, siRNA associated with carriers is usually taken up by endocytosis and travels through endosomal compartments before reaching lysosomes where it is subjected to degradation.[30,31] Therefore, researchers are dedicated to developing diversified gene carriers to facilitate the escape of siRNA from endosomes/lysosomes and protect the siRNA from degradation by lysosomal nucleases.[31−33] Guo *et al.*[22] deposited pH-sensitive molecules onto gold nanoparticles, achieving higher siRNA silencing efficacy than the vector designed by Elbakry *et al.*[21] However, the core of positively charged PEI/AuNP-MUA was fabricated using at least three steps, whereas the positive core of AuNP-CS was prepared in a single step. Schneider *et al.* reported that factors including the polyelectrolyte concentration, the contour length of the polyelectrolyte chain, and the ionic strength in solution could all contribute to nanoparticle aggregation during polyelectrolyte absorption, leading to low yield.[24] Therefore, reducing the number of assembly steps could increase the yield of layer-by-layer assembly nanosystems without affecting gene delivery efficiencies. In this study, our simplified approach for constructing gene carriers is direct and facile, avoiding fluctuations during the assembly process and improving vehicle yields.

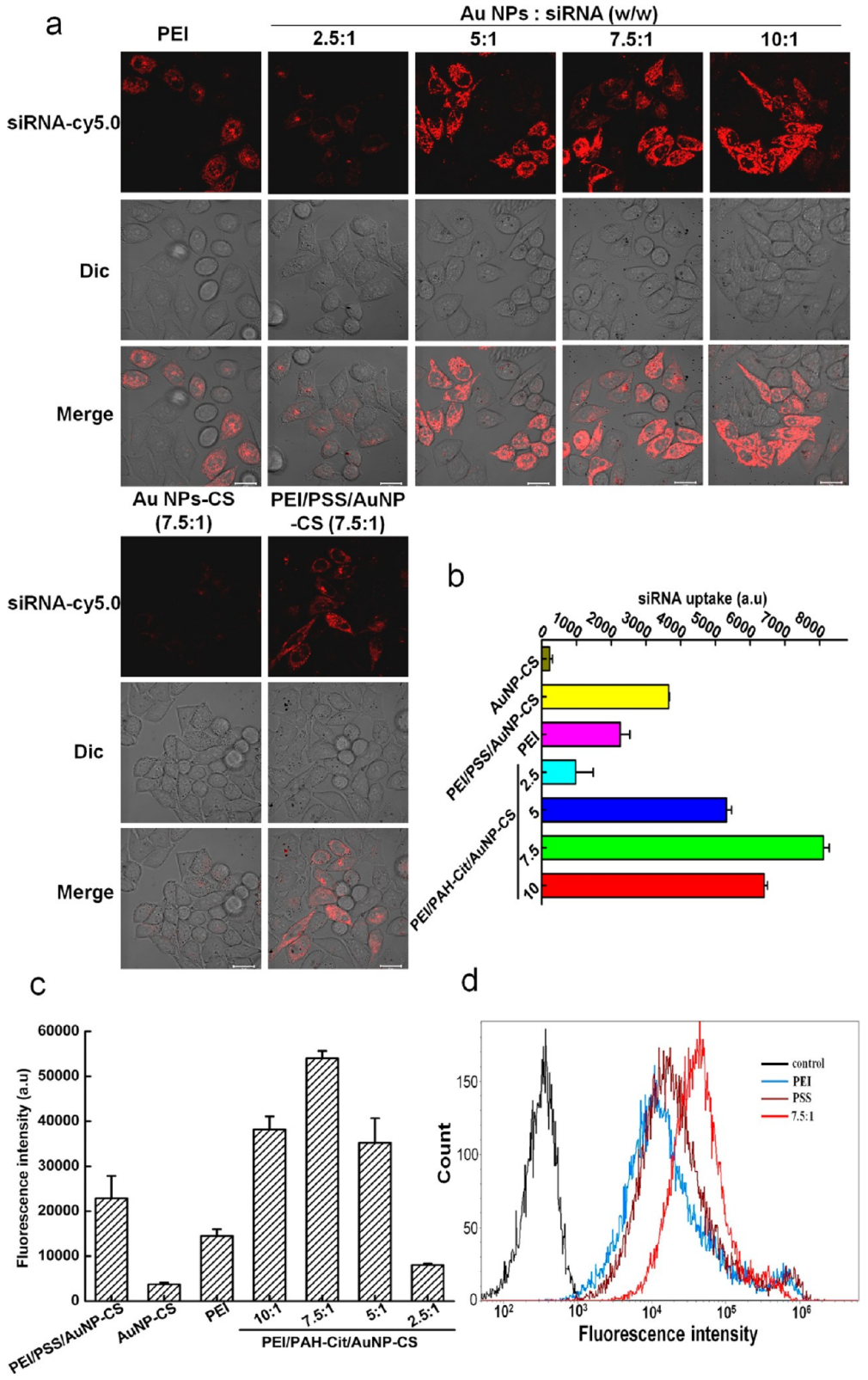

Figure 3. (a) Confocal microscope images of intracellular uptake of cy5-labeled siRNA (red) complexed with PEI, PEI/PAH-Cit/AuNP-CS at various vector/siRNA ratios (2.5:1, 5:1, 7.5:1, and 10:1), AuNP-CS, and PEI/PSS/AuNP-CS after incubation with HeLa cells for 24 h. Scale bar: 20 μm. (b) Quantitative analysis of cellular fluorescence of cy5-siRNA levels was performed using Image-Pro Plus software. (c) Fluorescence intensities of cy5-siRNA uptake by HeLa cells were determined by flow cytometry. (d) Histogram shows the cy5-siRNA fluorescence intensity in HeLa cells transfected with siRNA/PEI/PAH-Cit/AuNP-CS complex at a ratio of 7.5:1 for 24 h, with siRNA/PEI/PSS/AuNP-CS and siRNA/PEI as references.

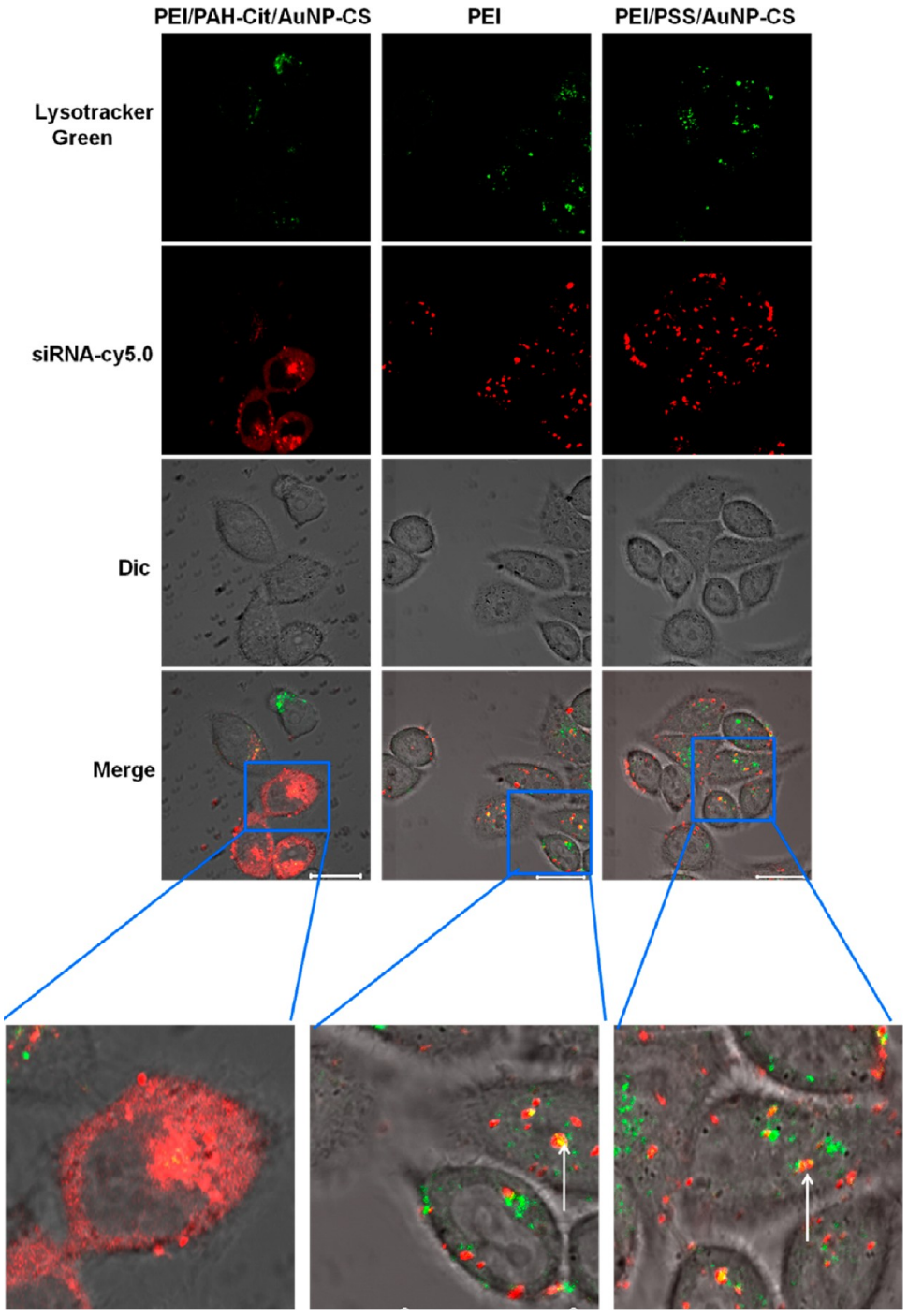

Figure 4. CLSM images of HeLa cells incubated with cy5-siRNA (red) complexed with PEI/PAH-Cit/AuNP-CS, PEI, and PEI/PSS/AuNP-CS for 6 h. Late endosomes and lysosomes were stained with lyso-tracker green (Molecular Probes, USA) for 30 min. Scale bar: 20 μm.

The biocompatibility of nonviral vectors is another crucial factor when designing nanosystems for nucleic acid delivery. Cytoplasmic PEI can initiate apoptosis by disrupting internal membranes, such as the mitochondrial membrane, endoplasmic reticulum, and Golgi apparatus;[27,34] consequently, lessening the PEI content of nanocarriers will reduce their cytotoxicity. Here, we prepared positively charged gold nanoparticles, which were reduced and stabilized by positively charged chitosan on the surface, as the core of a layer-by-layer assembly system to replace PEI deposited on AuNP-MUA cores. It is generally accepted that chitosan, a natural polysaccharide, is a biocompatible, biodegradable, and nontoxic material that is highly cationic and has the capacity to form polyelectrolyte complexes.[35] Our experimental results showed that PEI/PAH-Cit/AuNP-CS has good biocompatibility. We found that the viability of both HeLa and MCF-7R cells treated with

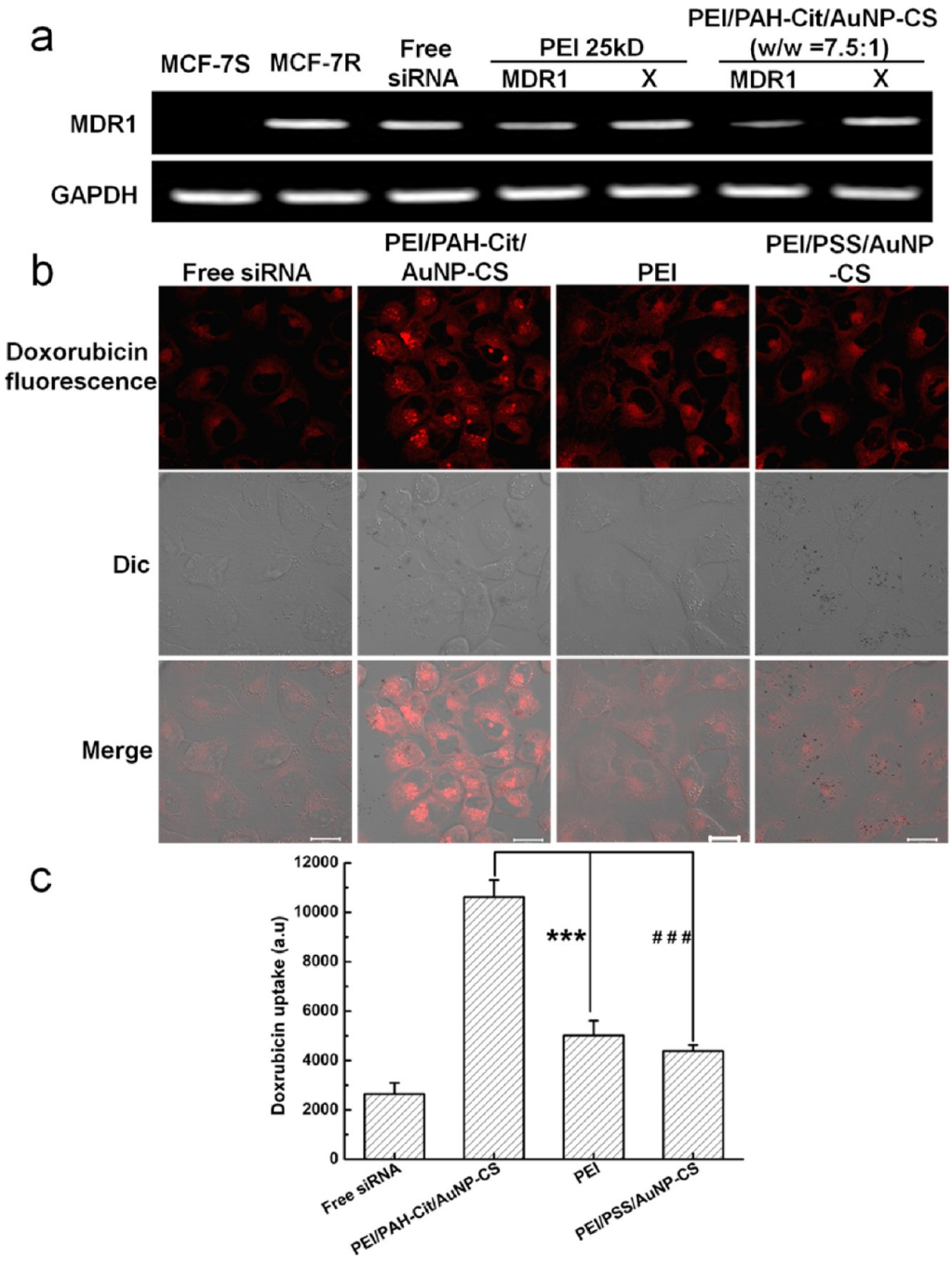

Figure 5. (a) *MDR1* knockdown efficacy detected by PCR. (b) CLSM images of MCF-7R cells incubated with naked *MDR1* targeted siRNA, PEI/PAH-Cit/AuNP-CS, PEI, and PEI/PSS/AuNP-CS complexed with *MDR1* targeted siRNA. MCF-7R cells were exposed to free siRNA or vector-complexed siRNA for 48 h, incubated with doxorubicin (red) for 24 h, and then subjected to CLSM imaging. Scale bar: 20 μm. (c) Quantitative analysis of intracellular doxorubicin uptake was executed by Image-Pro Plus software.

siRNA/PEI/PAH-Cit/AuNP-CS complexes was not reduced even though the mass ratio of the vector to siRNA reached 10:1 (Figure 2c). The benign biological responses of the cells toward AuNP-CS need to be investigated in depth.

High siRNA transfection efficiency is the most important factor in gene modification of cells. Naked, unmodified siRNAs cannot enter cells efficiently because the negative charges of their phosphodiester backbone lead to electrostatic repulsion from the anionic cell membrane surface and limit their permeability into cells. siRNA may be absorbed into the outer layer of PEI/PAH-Cit/AuNP-CS or may be present on the surface of the delivery vector, as indicated by the gel retardation assay (Figure 2a). The zeta-potential of complexes increased with the mass ratio of vector to siRNA (data not shown). Meanwhile, it is noteworthy that the highest delivery efficacy was observed at

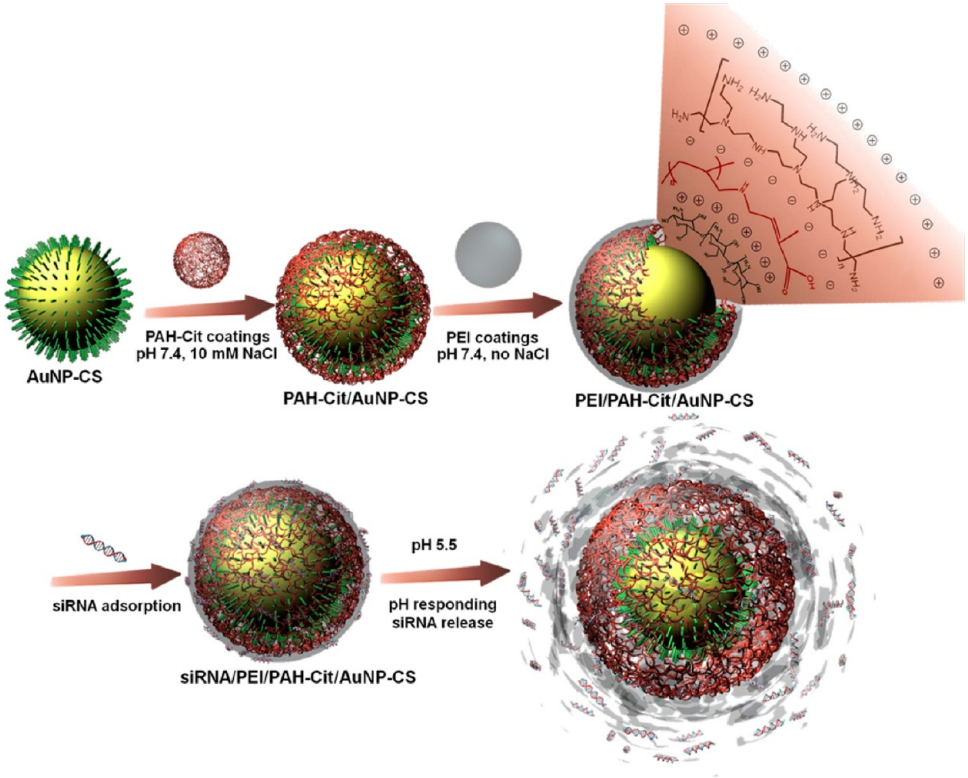

Scheme 1. Assembly steps for siRNA/PEI/PAH-Cit/AuNP-CS complexes and pH-responsive release of siRNA.

vector/siRNA ratios of 7.5 and 10. The cationic charges on the surfaces of these complexes may have enhanced their endocytosis.[36,37] In addition, a ratio of 7.5 gave a higher siRNA uptake and *MDR1* knockdown efficiency than a ratio of 10, which may indicate that excess PEI molecules can induce apoptosis or necrosis by disintegrating the cell membrane or disrupting internal organelles so that the cells are unable to produce normal biological responses.[27,38] Therefore, when designing new gene delivery systems, it is important to optimize the balance between polymer cationic density for effective gene transfer and low cytotoxicity.

Naked RNA molecules are very labile in acidic environments, for example, in late endosomes and lysosomes, where they can be destroyed by enzymatic degradation. It is generally accepted that the siRNA delivery efficacy is also related to the rate of intracellular degradation of siRNA. We showed here that the vector PEI/PAH-Cit/AuNP-CS protects siRNA from RNase degradation, which was further confirmed by competitive binding of SDS (Figure 2a). Moreover, compared to PEI/PSS/AuNP-CS, more absorbed siRNA was released from PEI/PAH-Cit/AuNP-CS at pH 5.5 (Figure 2b) or in endosomes (Figure 4). These results may suggest that the citraconic amide side chains of anionic charge-shifting polymer, PAH-Cit, were hydrolyzed under acidic conditions and changed to cationic PAH,[23] which destroyed the layer-by-layer structure of the vector and facilitated the release of the outer layer of PEI/siRNA. Moreover, the amino groups on PAH could contribute to the "proton-sponge" effect to promote disassociation of siRNA into the cytoplasm. The above-mentioned aspects may explain how PEI/PAH-Cit/AuNP-CS increases the uptake of cy5-siRNA and the efficiency of *MDR1* targeted siRNA knockdown.

The positive charges on the surface of siRNA/PEI/PAH-Cit/AuNP-CS complexes may interact with negatively charged biomolecules in the blood, which could inhibit its application *in vivo*. These negatively charged molecules, such as hyaluronic acid and transferrin, could be used as targeting molecules and be deposited on the surfaces of complexes with the siRNA, thus alleviating the adsorption of blood components and improving the accumulation of therapeutic siRNA in target tumors. A plethora of studies indicated that the extracellular pH (pHe) of most tumors is mildly acidic (pH > 6.5) and the pHe in only a small partion of tumor tissue is below 6.5.[42,43] The anionic charge-shifting polymer, PAH-Cit, is hardly hydrolyzed to cationic PAH. Therefore, in our subsequent job, the siRNA targeted apoptosis-related proteins (bcl-2, for instance) are delivered by PEI/PAH-Cit/AuNP-CS to inhibit the growth of nude mice bearing MCF-7R tumors (pH >6.5, as reported previously). We predicted that siRNA could not be released from the NPs in MCF-7R tumor region until the siRNA/vector complexes were endocytosed by tumor cells *via* the endosome/lysosome pathway, where the pH was 5.5 and finally siRNA was released into cytoplasm. In conclusion, this facile layer-by-layer assembly delivery system,

PEI/PAH-Cit/AuNP-CS, has the potential to be further exploited for *in vivo* application.

CONCLUSIONS

We prepared a pH-sensitive gene vehicle, PEI/PAH-Cit/AuNP-CS, using a facile layer-by-layer assembly method. This vector demonstrated high siRNA binding affinity and protected siRNA from enzyme degradation. At pH 5.5, the complex disassembled to release as much as 79% of the loaded siRNA during 4 h incubation time compared to only 23% at pH 7.4. As a toxicity-attenuated delivery carrier, PEI/PAH-Cit/AuNP-CS showed highest cy5-siRNA delivery efficacy in HeLa cells at a vector/siRNA w/w ratio of 7.5:1. Moreover, in MCF-7R cells, the targeted knockdown effect on *MDR1* mRNA expression was much higher than that of PEI using our new delivery carrier. The differential localization of cy5-siRNA and the lysosome marker lysotracker green indicates that most of the siRNA was specifically dispersed in cytoplasm due to the charge-reversal action of PAH-Cit. This research paves the way to prepare efficient gene nanocarriers using the facile layer-by-layer assembly approach and may be further exploited for clinical application.

EXPERIMENTAL SECTION

Materials. Branched PEI (25 kDa), PSS (70 kDa), PAH (15 kDa), chitosan (low molecular weight), and tetrachloroauric (III) acid were purchased from Sigma-Aldrich (St. Louis, MO). PAH-Cit was synthesized according to the reported procedure.[23] Dulbecco's modified Eagle's medium (DMEM), fetal bovine serum (FBS), ethidium bromide. and agarose were obtained from Invitrogen Corporation (Carlsbad, CA). Cy5-labeled siRNA was kindly donated by Professor Liang from Pecking University. The sequences were as follows: sense strand, 5′-UUCUCCGAACG-UGUCACGUdTdT-3′; antisense strand, 5′-ACGUGACACGUUCG-GAGAAdTdT-3′. The sense strand was labeled at the 5′ end with the cy5 fluorophore. The siRNA used for silencing the *MDR1* gene was purchased from Shanghai GenePharma Co., Ltd., and the sequences were as follows: sense strand, 5′-CGGAAGGC-CUAAUGCCGAAdTdT-3′; antisense strand, 5′-UUCGGCAUUAG-GCCUUCCGdTdG.-3′.

Synthesis of AuNP-CS. AuNP-CS was prepared as previously reported[39] with minor modifications. Briefly, 100 mL of 0.5% chitosan solution dissolved in 1% acetic acid was heated under reflux until boiling. Then, 425 μL of 1% $HAuCl_4 \cdot 3H_2O$ solution was added drop-by-drop with vigorous stirring. Boiling was continued for 15 min. The larger aggregates were removed using a 0.2 μm filter. The stabilized AuNP-CS was collected twice by centrifugation at 22 000*g*/min for 30 min and suspended in pH 8.0 NaOH solution, then centrifuged twice at 15 000*g*/min for 20 min. The collected AuNP-CS was dispersed in deionized water.

Assembly of siRNA/PEI/PAH-Cit/AuNP-CS Complexes. The complexes were assembled as illustrated in Scheme 1.[22] Crude PAH-Cit/AuNP-CS was precipitated by two rounds of centrifugation at 10 000*g*/min for 20 min and then resuspended in 10 mM HEPES buffer (pH 7.4) containing 10 mM NaCl. After PEI coating, PEI/PAH-Cit/AuNP-CS was collected twice at 5000*g*/min for 10 min and resuspended in 10 mM HEPES buffer without NaCl. To load siRNA onto the prepared vehicles, 1 μg/μL of siRNA solution in 10 mM sterile HEPES buffer was combined with PEI/PAH-Cit/AuNP-CS at various w/w ratios of Au to siRNA, and the weight of Au was calculated as reported.[40] The resulting mixtures were mixed by pipetting and incubated at room temperature for 30 min before use. The complex of siRNA with AuNP-CS or PEI/PSS/AuNP-CS was prepared similarly.

Characterization of PEI/PAH-Cit/AuNP-CS. Electron micrographs were obtained by a transmission electron microscope (TEM) (Tecnai G2 20 S-TWIN, FEI company, Hillsboro, OR). Samples were prepared by dipping 8 μL of Au colloidal solution onto a carbon-coated copper grid and air-dried before taking images. For negative staining, a copper grid, prepared as described above, was deposited in a uranyl acetate aqueous solution (0.1%, w/v) for 5 min. Before sampling, excess negative solution on the grid was wiped off using a filter paper, and residual solution was air-dried.

UV/vis spectra were recorded on a lambda 950 UV/vis/NIR spectrophotometer in the range of 400−700 nm. Zeta-potential was determined on a Nano-ZS (Malvern, Worcestershire, UK) Zetasizer at a scattering angle of 173° and analyzed using DTS (nano) program.

Evaluation of the Retardation and Protection of siRNA by the Complexes. First, 7.5 μL of siRNA/PEI/PAH-Cit/AuNP-CS complexes at various ratios from 0.63 to 10 in pH 7.4 HEPES buffer and 2.5 μL of 80% glycerol were mixed and subjected to 2% agarose gel electrophoresis containing 0.5 μg/mL ethidium bromide per well. Electrophoresis was carried out at a voltage of 110 V for 20 min in TBE running buffer.

To evaluate the protection of siRNA by PEI/PAH-Cit/AuNP-CS, 2 μL of RNaseA (5 U/μL) was used to digest 0.5 μg of siRNA formulated with PEI/PAH-Cit/AuNP-CS at 37 °C for 1 h. After digestion, 5 μL of 2% SDS was added to dissociate siRNA from the complexes. Images were recorded by Image Quant 300 (GE Healthcare, America).

siRNA Release from the Complexes. To measure the release profile of siRNA, PEI/PAH-Cit/AuNP-CS or PEI/PSS/AuNP-CS was complexed with siRNA at a w/w ratio of 7.5 in 10 mM HEPES buffer at either pH 5.5 or 7.4 and incubated in a 96-well culture plate at 37 °C. Samples were taken from the plate at scheduled time points and centrifuged at 5000*g* for 10 min, and the concentration of siRNA in 1 μL of supernatant was measured using an ES-2 spectrophotometer (e-spect, Malcom, Japan).

CCK-8 Assay. The proliferation of HeLa and MCF-7R cells in the presence of siRNA/PEI/PAH-Cit/AuNP-CS complexes was determined using a cell counting kit-8 (CCK-8, Dojindo Laboratories, Kumamoto, Japan). Specifically, HeLa or MCF-7R cell suspensions (100 μL, 1 $\times$ 10^4 cells per well) were dispensed into a 96-well plate and allowed to adhere overnight at 37 °C. Cells in each well were transfected with complexes containing 0.125 μg of siRNA in opti-MEM for 4 h, then the medium was changed to complete culture medium, and culture continued for another 44 h. Ten microliters of thawed CCK-8 solution was added to each well and incubated for 2 h, after which the absorbance was recorded at 450 nm with a reference wavelength of 630 nm. All data were presented as mean percentages $\pm$ SEM in triplicate compared to the OD values of nontreated cells.

Cellular Uptake. The cellular uptake of siRNA delivered by PEI/PAH-Cit/AuNP-CS was examined by confocal microscopy and flow cytometry. HeLa cells were plated in confocal dishes at a concentration of 2 $\times$ 10^5 cells per dish for 12 h before transfection. The complexes containing 2 μg of cy5-siRNA were incubated with HeLa cells according to the procedure described in the previous paragraph. Subsequently, the distribution of siRNA in cells was examined using Zeiss confocal microscopy (LSM700, Carl Zeiss, Germany). The transfected cells were collected and washed in PBS three times, and then the fluorescence intensity of cy5-siRNA was determined using an Attune acoustic focusing cytometer (Applied Biosystems, Life Technologies, Carlsbad, CA). It was supported with the joint lab of nanotechnology for bioapplication, which was established with Life Technologies Corp. in the National Center for Nanoscience and Technology of China.

Gene Silencing Efficiency. MCF-7R cells were plated in a 12-well plate (1 $\times$ 10^5 cells per well) and transfected as described above.

After transfection for 48 h, total RNA was isolated with Trizol reagent (Invitrogen, USA) and quantified by UV/vis spectroscopy at 260 nm. The reverse transcription reaction was performed using PrimeScript 1st Strand cDNA Synthesis Kit (TaKaRa Bio Inc., Japan). The newly synthesized cDNA was amplified by PCR. The reaction mixture contained cDNA template, PCR master mix buffer (Go Taq Colorless Master Mix, Promega), and *MDR1* primers (forward, 5- GTC CCA GGA GCC CAT CCT-3; reverse, 5-CCC GGC TGT TGT CTC CAT A-3[41]). GAPDH primers (forward, 5-GACTTCAACAGCAACTCCCAC-3; reverse, 5-TCCACCACCCTGTTGCTGTA-3) were used as an internal control. The cycling procedure was as follows: 94 °C for 2 min, then 29 cycles at 94 °C for 15 s, 55 °C for 20 s, 72 °C for 25 s, followed by 72 °C for 3 min. Aliquots of PCR products were resolved on a 1% agarose gel prestained with ethidium bromide.

To determine the effect of *MDR1* gene silencing on cellular uptake of doxorubicin, MCF-7R cells were placed into confocal dishes and transfected with *MDR1* siRNA/PEI/PAH-Cit/AuNP-CS for 48 h. Subsequently, cells were treated with 10 μg/mL dox for 4 h, and after washing the cells in cold PBS, accumulation of intracellular dox was examined using a Zeiss confocal microscopy.

Conflict of Interest: The authors declare no competing financial interest.

Acknowledgment. This work was financially supported in part by grants from the China Postdoctoral Science Foundation (No. Y1321Z11GJ), Chinese Natural Science Foundation project (No. 30970784 and 81171455), National Key Basic Research Program of China (2009CB930200), Chinese Academy of Sciences (CAS) "Hundred Talents Program" (07165111ZX), and CAS Knowledge Innovation Program and Research Fund for the Doctoral Program of Higher Education of China (No. 20111301110004).

REFERENCES AND NOTES

1. de Fougerolles, A.; Vornlocher, H.-P.; Maraganore, J.; Lieberman, J. Interfering with Disease: A Progress Report on siRNA-Based Therapeutics. *Nat. Rev. Drug Discovery* **2007**, *6*, 443–453.
2. Oh, Y.-K.; Park, T. G. siRNA Delivery Systems for Cancer Treatment. *Adv. Drug Delivery Rev.* **2009**, *61*, 850–862.
3. Sonawane, N. D.; Szoka, F. C.; Verkman, A. S. Chloride Accumulation and Swelling in Endosomes Enhances DNA Transfer by Polyamine-DNA Polyplexes. *J. Biol. Chem.* **2003**, *278*, 44826–44831.
4. Xue, H.-Y.; Wong, H.-L. Solid Lipid−PEI Hybrid Nanocarrier: An Integrated Approach To Provide Extended, Targeted, and Safer siRNA Therapy of Prostate Cancer in an All-in-One Manner. *ACS Nano* **2011**, *5*, 7034–7047.
5. Park, J. S.; Yang, H. N.; Woo, D. G.; Jeon, S. Y.; Do, H. J.; Lim, H. Y.; Kim, J. H.; Park, K. H. Chondrogenesis of Human Mesenchymal Stem Cells Mediated by the Combination of SOX Trio SOX5, 6, and 9 Genes Complexed with PEI-Modified PLGA Nanoparticles. *Biomaterials* **2011**, *32*, 3679–3688.
6. Takahashi, Y.; Nishikawa, M.; Takakura, Y. Nonviral Vector-Mediated RNA Interference: Its Gene Silencing Characteristics and Important Factors To Achieve RNAi-Based Gene Therapy. *Adv. Drug Delivery Rev.* **2009**, *61*, 760–766.
7. Toh, E. K.-W.; Chen, H.-Y.; Lo, Y.-L.; Huang, S.-J.; Wang, L.-F. Succinated Chitosan as a Gene Carrier for Improved Chitosan Solubility and Gene Transfection. *Nanomed. Nanotechnol.* **2011**, *7*, 174–183.
8. Tros de Ilarduya, C.; Sun, Y.; Düzgünes, N. Gene Delivery by Lipoplexes and Polyplexes. *Eur. J. Pharm. Sci.* **2010**, *40*, 159–170.
9. Morille, M.; Passirani, C.; Dufort, S.; Bastiat, G.; Pitard, B.; Coll, J. L.; Benoit, J. P. Tumor Transfection after Systemic Injection of DNA Lipid Nanocapsules. *Biomaterials* **2011**, *32*, 2327–2333.
10. O'Rorke, S.; Keeney, M.; Pandit, A. Non-viral Polyplexes: Scaffold Mediated Delivery for Gene Therapy. *Prog. Polym. Sci.* **2010**, *35*, 441–458.
11. Chen, B.; Liu, M.; Zhang, L.; Huang, J.; Yao, J.; Zhang, Z. Polyethylenimine-Functionalized Graphene Oxide as an Efficient Gene Delivery Vector. *J. Mater. Chem.* **2011**, *21*, 7736–7741.
12. Tsai, L. R.; Chen, M. H.; Chien, C. T.; Chen, M. K.; Lin, F. S.; Lin, K. M. C.; Hwu, Y. K.; Yang, C. S.; Lin, S. Y. A Single-Monomer Derived Linear-like PEI-*co*-PEG for siRNA Delivery and Silencing. *Biomaterials* **2011**, *32*, 3647–3653.
13. Yang, H. N.; Park, J. S.; Woo, D. G.; Jeon, S. Y.; Do, H.-J.; Lim, H.-Y.; Kim, J.-H.; Park, K.-H. C/EBP-[alpha] and C/EBP-[beta]-Mediated Adipogenesis of Human Mesenchymal Stem Cells (hMSCs) Using PLGA Nanoparticles Complexed with Poly(ethyleneimmine). *Biomaterials* **2011**, *32*, 5924–5933.
14. Decher, G.; Hong, J.-D. Buildup of Ultrathin Multilayer Films by a Self-Assembly Process, 1 Consecutive Adsorption of Anionic and Cationic Bipolar Amphiphiles on Charged Surfaces. *Makromol. Chem. Macromol. Symp.* **1991**, *46*, 321–327.
15. Bricaud, Q.; Fabre, R. M.; Brookins, R. N.; Schanze, K. S.; Reynolds, J. R. Energy Transfer between Conjugated Polyelectrolytes in Layer-by-Layer Assembled Films. *Langmuir* **2011**, *27*, 5021–5028.
16. Lee, S. K.; Han, M. S.; Asokan, S.; Tung, C.-H. Effective Gene Silencing by Multilayered siRNA-Coated Gold Nanoparticles. *Small* **2011**, *7*, 364–370.
17. Ghosh, P.; Han, G.; De, M.; Kim, C. K.; Rotello, V. M. Gold Nanoparticles in Delivery Applications. *Adv. Drug Delivery Rev.* **2008**, *60*, 1307–1315.
18. Pissuwan, D.; Niidome, T.; Cortie, M. B. The Forthcoming Applications of Gold Nanoparticles in Drug and Gene Delivery Systems. *J. Controlled Release* **2011**, *149*, 65–71.
19. Ghosh, P. S.; Kim, C. K.; Han, G.; Forbes, N. S.; Rotello, V. M. Efficient Gene Delivery Vectors by Tuning the Surface Charge Density of Amino Acid-Functionalized Gold Nanoparticles. *ACS Nano* **2008**, *2*, 2213–2218.
20. Lee, J. S.; Green, J. J.; Love, K. T.; Sunshine, J.; Langer, R.; Anderson, D. G. Gold, Poly(β-amino ester) Nanoparticles for Small Interfering RNA Delivery. *Nano Lett.* **2009**, *9*, 2402–2406.
21. Elbakry, A.; Zaky, A.; Liebl, R.; Rachel, R.; Goepferich, A.; Breunig, M. Layer-by-Layer Assembled Gold Nanoparticles for siRNA Delivery. *Nano Lett.* **2009**, *9*, 2059–2064.
22. Guo, S.; Huang, Y.; Jiang, Q.; Sun, Y.; Deng, L.; Liang, Z.; Du, Q.; Xing, J.; Zhao, Y.; Wang, P. C. Enhanced Gene Delivery and siRNA Silencing by Gold Nanoparticles Coated with Charge-Reversal Polyelectrolyte. *ACS Nano* **2010**, *4*, 5505–5511.
23. Liu, X.; Zhang, J.; Lynn, D. M. Polyelectrolyte Multilayers Fabricated From Charge-Shifting Anionic Polymers: A New Approach to Controlled Film Disruption and the Release of Cationic Agents from Surfaces. *Soft Matter* **2008**, *4*, 1688–1695.
24. Schneider, G.; Decher, G. Functional Core/Shell Nanoparticles *via* Layer-by-Layer Assembly. Investigation of the Experimental Pparameters for Controlling Particle Aggregation and for Enhancing Dispersion Stability. *Langmuir* **2008**, *24*, 1778–1789.
25. Mayya, K. S.; Schoeler, B.; Caruso, F. Preparation and Organization of Nanoscale Polyelectrolyte-Coated Gold Nanoparticles. *Adv. Funct. Mater.* **2003**, *13*, 183–188.
26. Lee, L.; Cavalieri, F.; Johnston, A. P. R.; Caruso, F. Influence of Salt Concentration on the Assembly of DNA Multilayer Films. *Langmuir* **2009**, *26*, 3415–3422.
27. Parhamifar, L.; Larsen, A. K.; Hunter, A. C.; Andresen, T. L.; Moghimi, S. M. Polycation Cytotoxicity: A Delicate Matter for Nucleic Acid Therapy-Focus on Polyethylenimine. *Soft Matter* **2010**, *6*, 4001–4009.
28. Poma, P.; Notarbartolo, M.; Labbozzetta, M.; Maurici, A.; Carina, V.; Alaimo, A.; Rizzi, M.; Simoni, D.; D'Alessandro, N. The Antitumor Activities of Curcumin and of Its Isoxazole Analogue Are Not Affected by Multiple Gene Expression Changes in an MDR Model of the MCF-7 Breast Cancer Cell Line: Analysis of the Possible Molecular Basis. *Int. J. Mol. Med.* **2007**, *20*, 329.
29. Poon, Z.; Chang, D.; Zhao, X.; Hammond, P. T. Layer-by-Layer Nanoparticles with a pH-Sheddable Layer for *In Vivo*

Targeting of Tumor Hypoxia. *ACS Nano* **2011**, *5*, 4284–4292.
30. Wattiaux, R.; Laurent, N.; Wattiaux-De Coninck, S.; Jadot, M. Endosomes, Lysosomes: Their Implication in Gene Transfer. *Adv. Drug Delivery Rev.* **2000**, *41*, 201–208.
31. Kakimoto, S.; Hamada, T.; Komatsu, Y.; Takagi, M.; Tanabe, T.; Azuma, H.; Shinkai, S.; Nagasaki, T. The Conjugation of Diphtheria Toxin T Domain to Poly(ethylenimine) Based Vectors for Enhanced Endosomal Escape during Gene Transfection. *Biomaterials* **2009**, *30*, 402–408.
32. You, J. O.; Auguste, D. T. The Effect of Swelling and Cationic Character on Gene Transfection by pH-Sensitive Nanocarriers. *Biomaterials* **2010**, *31*, 6859–6866.
33. Miyata, K.; Oba, M.; Nakanishi, M.; Fukushima, S.; Yamasaki, Y.; Koyama, H.; Nishiyama, N.; Kataoka, K. Polyplexes from Poly(aspartamide) Bearing 1, 2-Diaminoethane Side Chains Induce pH-Selective, Endosomal Membrane Destabilization with Amplified Transfection and Negligible Cytotoxicity. *J. Am. Chem. Soc.* **2008**, *130*, 16287–16294.
34. Christy, H. Molecular Hurdles in Polyfectin Design and Mechanistic Background to Polycation Induced Cytotoxicity. *Adv. Drug Delivery Rev.* **2006**, *58*, 1523–1531.
35. Kean, T.; Thanou, M. Biodegradation, Biodistribution and Toxicity of Chitosan. *Adv. Drug Delivery Rev.* **2010**, *62*, 3–11.
36. Lee, J.-S.; Green, J. J.; Love, K. T.; Sunshine, J.; Langer, R.; Anderson, D. G. Gold, Poly(β-amino ester) Nanoparticles for Small Interfering RNA Delivery. *Nano Lett.* **2009**, *9*, 2402–2406.
37. Thibault, M.; Astolfi, M.; Tran-Khanh, N.; Lavertu, M.; Darras, V.; Merzouki, A.; Buschmann, M. D. Excess Polycation Mediates Efficient Chitosan-Based Gene Transfer by Promoting Lysosomal Release of the Polyplexes. *Biomaterials* **2011**, *32*, 4639–4646.
38. Putnam, D.; Gentry, C. A.; Pack, D. W.; Langer, R. Polymer-Based Gene Delivery with Low Cytotoxicity by a Unique Balance of Side-Chain Termini. *Proc. Natl. Acad. Sci. U.S.A.* **2001**, *98*, 1200.
39. Bhumkar, D. R.; Joshi, H. M.; Sastry, M.; Pokharkar, V. B. Chitosan Reduced Gold Nanoparticles as Novel Carriers for Transmucosal Delivery of Insulin. *Pharm. Res.* **2007**, *24*, 1415–1426.
40. Link, S.; El-Sayed, M. A. Spectral Properties and Relaxation Dynamics of Surface Plasmon Electronic Oscillations in Gold and Silver Nanodots and Nanorods. *J. Phys. Chem. B* **1999**, *103*, 8410–8426.
41. Wang, J.; Tao, X.; Zhang, Y.; Wei, D.; Ren, Y. Reversion of Multidrug Resistance by Tumor Targeted Delivery of Antisense Oligodeoxynucleotides in Hydroxypropyl-Chitosan Nanoparticles. *Biomaterials* **2010**, *31*, 4426–4433.
42. Volk, T.; Jähde, E.; Fortmeyer, H.; Glüsenkamp, K.; Rajewsky, M. pH in Human Tumour Xenografts: Effect of Intravenous Administration of Glucose. *Br. J. Cancer* **1993**, *68*, 492–500.
43. Engin, K.; Leeper, D.; Cater, J.; Thistlethwaite, A.; Tupchong, L.; McFarlane, J. Extracellular pH Distribution in Human Tumours. *Int. J. Hyperthermia* **1995**, *11*, 211–216.